Study of a Liquid-Vapour Ejector in the context of an advanced TPL ejector-absorption cycle working with a low temperature heat source and an ammonia-water mixture

Filipe Alexandre Ereira Mendes Marques*
Instituto Superior Técnico (IST), Portugal

May, 2009

Abstract

In this work, the limits of the use of a liquid-vapour ejector without phase change were studied for pressure recovery, in view of its introduction at the absorber inlet, in a single-stage absorption cycle working with a low temperature heat source and an ammonia-water mixture, therefore converting the cycle into an advanced TPL ejector-absorption cycle.

In order to find the possible pressure recovery and respective ejector design, within the desired cycle's working conditions, a new two-phase flow model for the liquid-vapour ejector was developed and applied as a simulation program. The model aims to expand the currently used models. It assumes the liquid phase in the form of droplets in the conical diffuser and includes interaction between phases, inertial effects and adds pressure losses due to friction, the binary mixture composition of ammonia-water for each phase and its variation with mass transfer, as well as the droplets diameter variation.

From the simulation of the mixing zone and the diffuser, it was found that the pressure recovery increases for lower diffuser angles, with a maximum pressure recovery of 0,05 *bar* for a tube, observing that the pressure recovery is fundamentally due to the mixture of the fluids. An high sensibility of the nozzle's outlet pressure with the diameter variation was observed and analysed.

In this specific case of the use of ammonia-water as the working mixture, it was found the need to expand the ejector's model to include phase change at the nozzle, in order to have significant pressure recover.

*Thesis advisor: Doutor Luis Filipe Mendes

1 Introduction

In sunny and warm countries like Portugal, one of the highest energy spending is on air conditioning and coolers during spring, summer and begins of autumn[1]. Absorption cooling technologies driven by thermal solar energy come up as promising alternatives to the conventional intensive electrical energy spending cooling technology.

One characteristic greatly responsible for slowing up the progress into market of absorption technologies is its lower efficiency compared to conventional technologies, which implies the use of large solar fractions in order to have comparable fossil primary energy consumption, *i.e.*, comparable CO_2 emissions [2]. Advanced absorption cycles are being studied in order to increase the *Coefficient of Performance* (*COP*) of this type of machines, as well as its adaptability and to widen the scope of its uses [3], [4].

One type of such advanced cycles is the *Triple Pressure Level cycle* (*TPL*), which consist of the conventional *Double Pressure Level* cycle (*DPL*) with an extra intermediate pressure level, achieved by means of a pump or pump like device. A jet pump or *Ejector* seems to be a very good solution to maintain the pressure difference, because it has no moving parts, requires low maintenance, do not need an additional energy source, as it uses energy otherwise lost in the cycle, and it is cost effective.

1.1 Motivation

The motivation for the present work is to convert an existing DPL single-stage absorption refrigeration cycle, applied in a Lab prototype chiller working with a mixture of ammonia-water and low temperature heat input at the LSAS[1] in IST, into a TPL ejector-absorption cycle, in view of decreasing the generator temperature while maintaining or increasing the COP and thus, obtaining higher solar fractions.

1.2 Objective

The objective of this work is the study of the limits of the use of a liquid-vapour ejector (without phase change) for pressure recovery at the absorber, converting the single-stage DPL absorption cycle in a TPL ejector-absorption cycle, since this is the type of ejector usually used in that cycle configuration [3], [4].

1.3 Liquid-Vapour Ejector

The *Ejector* is a device that uses the energy of one fluid, *the motive fluid*, for suction and entrainment of another fluid, *the affected fluid*, followed by a final re-compression of the two fluid mixture exiting the ejector.

The device (see Fig.1) is composed by three components: the *Injector*, with an internal nozzle, where the motive flow is accelerated and pressure energy is

[1] Laboratorio de Sistemas de Arrefecimento Solar

converted into kinetic energy; the *Mixture Zone*, where suction occurs and both fluids meet; and the *Diffuser*, where there is further mixing of the fluids and compression;

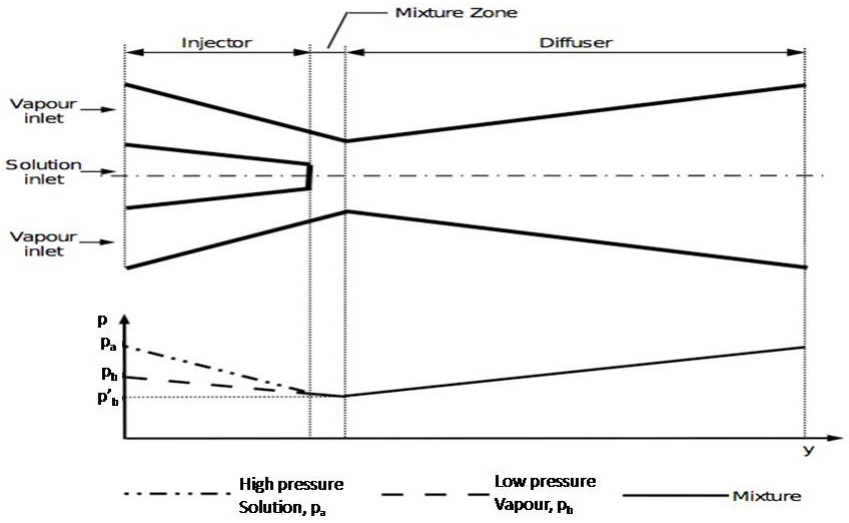

Figure 1: Ejector's scheme over a graph of the ejector's pressure variation along the length.

1.4 TPL ejector-absorption cycle

A TPL cycle by means of an ejector is called an *advanced ejector-absorption cycle*. There are different ejector-absorption cycles according to different motivations[3], [4]. The ejector-absorption cycle that suits the above motivation is obtained from a single-stage absorption cycle, introducing a specifically designed liquid-vapour ejector at the absorber inlet (see Fig.2) for pressure recovery and pre-compression. In this cycle, the jet ejector receives the high pressure weak solution returning from the generator through the solution heat exchanger, which uses as the motive fluid (energy input) to entrain the low pressure refrigerant vapour coming from the evaporator through the refrigerant heat exchanger, being the resulting mixture discharged into the absorber at an intermediate pressure.

There are two desired effects resulting from this cycle (see Fig.3), which yield an improvement of the cycle performance [5],[6]:

- The ability to lower the generator temperature, T_g. If the evaporator and cooling-water temperatures (condenser and absorber temperature), and f remain the same, the higher absorber pressure for the TPL cycle means

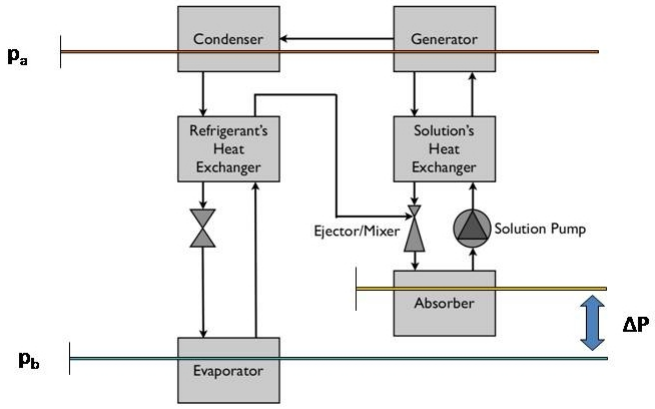

Figure 2: Triple-pressure-level single-stage advanced absorption cycle.

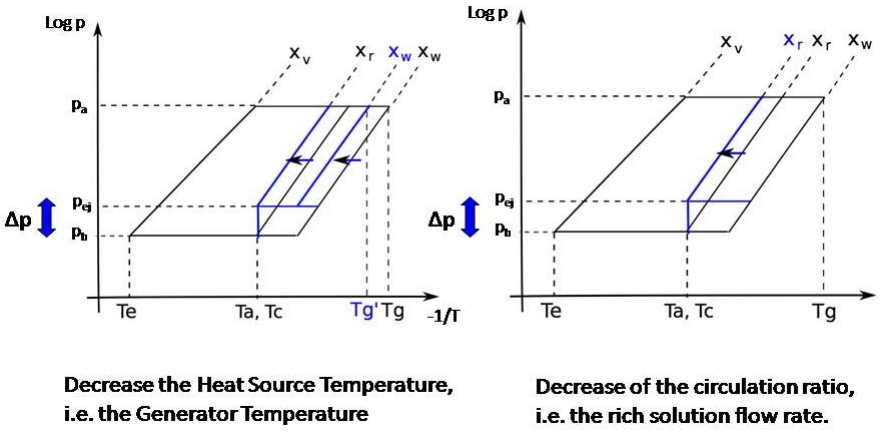

Figure 3: PT Diagram showing the effects of the introduction of the ejector in the common DPL cycle.

a lower generator temperature, and thus a lower temperature heat source can be used more efficiently with the TPL cycle.

- The ability to decrease the circulation ratio, *f*. If the governing cycle temperatures (evaporator, generator and cooling-water) remain the same, the higher absorber pressure for the TPL cycle at the same absorber outlet temperature results in a higher mass fraction of the refrigerant in the solution. Such an increase of the rich solution means a decrease in the circulation ratio, *f*, given by

$$f = \frac{\dot{\mathcal{M}}_{rich}}{\dot{\mathcal{M}}_{refrigerant}} = \frac{x_{refrigerant} - x_{weak}}{x_{rich} - x_{weak}} \tag{1}$$

  Hence, a lower mass flow rate of the rich solution is needed for the same quantity of refrigerant and there is a reduction of the irreversibilities due to the heat transferred from the generator and the absorber.

These effects, the ability to lower the generator temperature and the circulation ratio, were previously studied by Gonçalves[6] for the same cycle in this work, who observed an increase in the COP and in the efficiency if the solar collectors, which makes the TPL cycle specially suited for the use of solar energy.

2 Method

To find the maximum pressure recovery possible within the current working conditions of the referred existing absorption chiller, and respective ejector design conditions, a new two-phase flow model for the liquid-vapour ejector was developed, and a parametric simulation of the ejector was carried out under the chiller's design conditions, within the EES programming environment.

The ejector was simulated for the current chiller's design conditions, which impose initial and boundary conditions, both to the geometry and state variables of the device, described in annex B.

2.1 Model of the Ejector

A new model of the flow in the Ejector was derived considering differential control volumes. The model is subdivided according to the ejectors components: the liquid flow of the motive fluid in the nozzle; the mixing of the fluids at the mixing zone; the two-phase flow of the mixture at the diffuser;

The control volumes considered are shown in Fig.4.

The following assumptions were made to characterize the ejector's flow:

1. $\partial/\partial t = 0$, **steady** flow (completely developed, variations with time are negligible).

2. $Q = 0$, **adiabatic** control volume (there is no energy transferred through the walls).

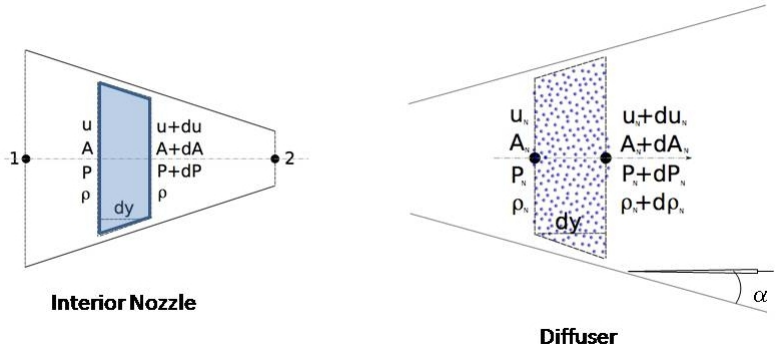

Figure 4: Control Volumes used for the flow model in the ejector.

3. $\partial/\partial r \sim 0$ and $\partial/\partial\beta \sim 0$, **one-dimensional** flow (symmetry around the axis, properties vary only with y).
4. **negligible gravity** influence (not worth considering / dimensionally insignificant for the problem).
5. **incompressible liquid phase**.
6. Liquid flow in the form of droplets inside the diffuser, with average diameter, and no interaction between each droplets, nor with the wall.

Mass, momentum and energy interactions between the phases were considered, as well as the refrigerant's mass fraction and the droplets diameter variation with the mass transfer, and the friction losses.

Annex A shows the formulae for the model.

3 Simulation Results and Discussion

Before the two-phase simulation of the ejector, the flow of the vapour alone in the diffuser was simulated in order to find what pressure could the vapour recover by itself and test the program. The maximum pressure recovered in the simulation was in close agreement with the theoretical result, with a small difference expected due to the compressibility and friction effects. The maximum pressure recoverable in theory is:

$$\Delta p = \frac{\rho\ u^2}{2} \ = \ 1,4\ mbar \tag{2}$$

The weight of the pressure recovery on the DPL pressure differential is defined as:

$$\Delta p_{\%} \equiv \frac{\Delta p - (p_b - p_{b'})}{p_a - p_b} = \frac{\rho\ u^2}{2(p_a - p_b)} \ = \ \frac{0,0014}{15,7 - 5,6}(\times 100) = 0,014\% \tag{3}$$

Therefore, the vapour alone has not enough energy available to recover pressure by itself. It is expected that most of the pressure recovery will be due to the energy transferred by the motive fluid as the next results will show.

3.1 Simulation of the ejector

The pressure recovery resulting of the simulation of the ejector for different diffuser angles, is shown in Fig.5 for the first 20 cm [2]. The ejector was simulated until one meter, however the maximum pressure recovery is achieved in the first 20 cm, and no other relevant information is contained in the remaining length of the diffuser besides the friction losses.

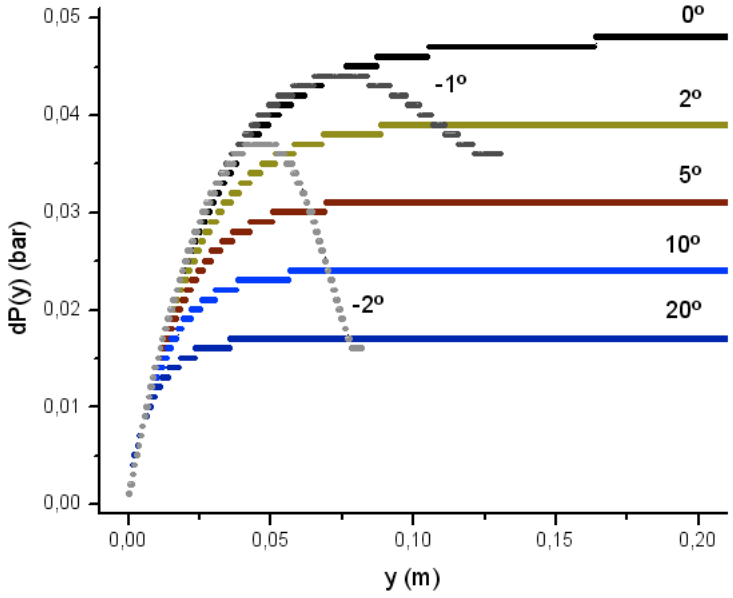

Figure 5: Pressure recovery for the first 20cm of the diffuser's length for different diffuser angles.

It is observed that the pressure recovery is mainly due to the momentum transfer by the droplets and the maximum recovery is achieved when the relative velocity between the phases is null. The pressure recovery increases for

[2]The results presented are the difference of the local pressure in the diffuser and the low initial pressure, i.e. the pressure recovered. The stair type lines of the figure are a result of the observed lower pressure recovery than expected. The output of the pressure results to a data file was less precise than needed for a smooth plot of the low pressure difference along the diffuser, and each level step represent the transition to a higher integer value of the lower decimal place of the output pressure printed in the file. However, the resulting graphs are sufficient to extract and represent the needed information for this work.

lower diffuser angle and the maximum pressure recovery is 48 *mbar* for a tube, representing 0,5%. To have a significant impact on the machine, the pressure recovery would have to be one order of greatness higher [6].

Another interesting result from the simulation is the pressure variation along the nozzle as a function of the diameter, presented in Fig.6. It is observed that the desired pressure for the vapour coming from the evaporator, that is, the desired pressure at the outlet of the nozzle, is very near the vapour's pressure, when phase change would occur. A decrease of just tens of micrometers would mean that phase change would occur inside the nozzle, which lies outside this ejector's model and the aim of this study. A question arises from this results on the effects of letting phase change occur inside the interior nozzle. Allowing a lower pressure for the vapour coming from the evaporator, and then phase change inside the interior nozzle, will allow the motive flow to achieve higher velocities and a higher entrainment of the affected flow, i.e. higher interaction surface between the fluids.

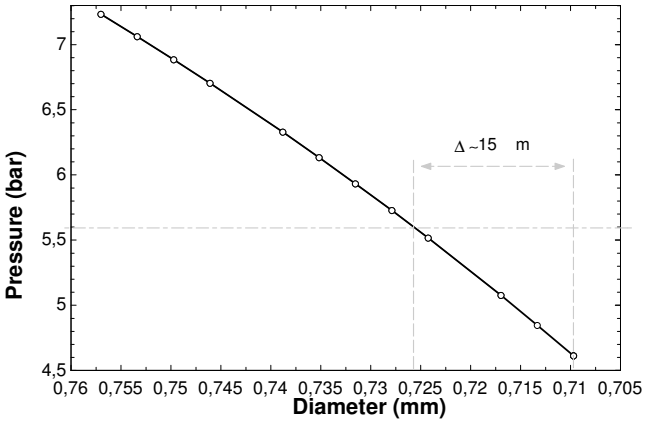

Figure 6: Pressure inside the interior nozzle as a function of the diameter along the length of the nozzle, with friction. This presents in detail the pressure variation with diameter around the desired low pressure point of work marked by the gray line. The interval indicated is the diameter variation between the one corresponding to the desired pressure, and the corresponding to the pressure at which phase change starts.

4 Conclusions

A new two-phase flow model was derived for a liquid-vapour ejector without phase change inside the nozzle. The model adds to previous ejectors models used in this kind of simulations the mechanical energy losses due to friction with the wall, which reduce the available energy for pressure recovery through dissipation along the way, particularly yielding a maximum on the tube's pressure recovery profile. The diffuser's model includes the mass, momentum and energy transfer between the phases (for different kinetic regimes), as well as inertial forces associated with the flow. Beside this quantities also considered in previous models, the new model takes into account the vapour's refrigerant mass fraction in the calculations of its physical and state properties, as well as the change of the mass fraction of the phases and the variation of the droplet diameter with the mass transference.

A simulation of the ejector was then carried out based on the new model developed. The program was used to study the pressure recovery possible for an ejector working in an ejector-absorption cycle with low temperature heat source and a binary mixture of ammonia-water, adding new simulation results for this specific type of ejector-absorption cycles to the results of ejector-absorption cycles that exist in literature. It was concluded that the pressure recovery possible increased with the decrease of the diffuser angle. The simulation yielded a maximum pressure recovery possible of 0,05 bar for a tube with a $20cm$ length, which is too low to have a noticeable impact on the machine's efficiency. It was also observed that the outlet pressure of the nozzle, i.e. the low pressure, is near the vapour pressure for the motive flow state conditions. A question arises from this results concerning the effects of letting phase change occur inside the interior nozzle.

The simulation provided useful insight on the diffuser's multiphase flow. The introduction of the friction made possible to account for pressure loss with the length, resulting in a well defined maximum pressure recovery point for the tube. It was concluded that the dominant force for pressure recovery in such systems is the momentum transfer, and that the assumption of constant pressure along the length of a mixing chamber is not valid.

It was concluded that it is favorable to expand the model of the liquid-vapour ejector to include phase change inside the injector, for the case of using ammonia-water as the working mixture.

Such a liquid-vapour ejector model that includes phase change in the nozzle have not been read neither referred in the bibliography. Therefore, the prosecution of the work initiated in this dissertation, includes the derivation of a new theoretical flow model for the liquid-vapour ejector including phase change at the injector, as well as its experimental validation.

References

[1] Pons M. et al. Thermodynamic based comparison of sorption systems for cooling and heat pumping. *International Journal of Refrigeration*, 22(1):5–7, 1999.

[2] L. Filipe Mendes, M. Collares-Pereira, and F. Ziegler. Supply of cooling and heating with solar assisted absorption heat pumps: an energetic approach. *International Journal of Refrigeration*, 21(2):116–125, March 1998.

[3] Shenyi Wu and Ian W. Eames. Innovations in vapour-absorption cycles. *Applied Energy*, 66(3):251–266, July 2000.

[4] Pongsid Srikhirin, Satha Aphornratana, and Supachart Chungpaibulpatana. A review of absorption refrigeration technologies. *Renewable and Sustainable Energy Reviews*, 5(4):343–372, December 2001.

[5] A. Levy, M. Jelinek, and I. Borde. Performance of a triple-pressure-level absorption cycle with r125-n,n'-dimethylethylurea. *Applied Energy*, 71:171–189, 2002.

[6] A. C. Gonçalves. *Estudo e Concepção de um Ejector para uma Máquina de Absorção com o par NH_3/H_2O*. Instituto Superior Técnico - UTL, Lisboa, Portugal, Setembro 2006.

[7] Frank P. Incropera and David P. Dewitt. *Fundamentos de Transferência de Calor e Massa*. LTC Editora (Authorized translation from the english edition published by John Wiley & Sons, Inc.), 5th edition, 2003.

[8] Christopher Earls Brennen. *Fundamentals of Multiphase Flow*. Cambridge University Press, 2005.

A Flow Model

Nomenclature

- A Cross Section Area $[m^2]$
- D Diameter $[m]$
- $\mathcal{D}$ Diffusion coefficient $[m^2/s]$
- $\hat{e}$ Specific internal energy $[J/kg]$
- e Specific energy $[J/kg]$
- f Darcy friction factor
- F Force related to momentum transfer between phases
- h Specific enthalpy $[J/kg]$
- k thermal conductivity $[J\ K^{-1}m^{-1}s^{-1}]$
- $\dot{\mathcal{M}}$ Mass flow rate $[kg/s]$
- $\dot{M}$ Moment flow rate $[N]$
- n Number of droplets per unit of control volume
- p Pressure $[Pa]$
- $\dot{Q}$ Heat power transferred between phases $[W]$
- Re Reynolds Number of the droplet
- T Temperature $[K]$
- u Cross section's mean velocity $[m/s]$
- x Ammonia's mass fraction. $[kg/kg]$
- y Length parallel with the axis of the diffuser or nozzle in the flow direction. $[m]$
- w specific work. $[J/kg]$
- $\dot{W}$ Power relative to the work done by transfer forces. $[W]$

Greek letters

- ϵ Mean Phase content $[m^3/m^3]$
- ν Kinetic viscosity. $[m^2s^{-1}]$
- ρ Density $[kg/m^3]$
- τ Shear-Stress $[kg/m^3]$
- ξ Weight of the mass transfer flow rate on the mass flow rate $[(kg/m^3)/(kg/m^3)]$

Subscripts

- N General Phase.
- C Continuous Phase.
- D Disperse Phase.
- DC Relative difference of a quantity in phase D to the same quantity in phase C.
- $\rightarrow$ N Quantity Transferred to Phase N.
- δ Relative to the droplet.

Model

The mass, momentum and energy equations for the flow model of the nozzle are:

$$\frac{dA}{A} + \frac{du}{u} = 0 \tag{4}$$

$$dx = 0 \tag{5}$$

$$\frac{dp}{\rho} + udu + f\frac{u^2}{2}\frac{dy}{D} = 0 \tag{6}$$

$$d\hat{e} - w_\tau = f\frac{u^2}{2}\frac{dy}{D} \tag{7}$$

where the friction term per differential control volume was approximated to that of a tube with the initial diameter of the control volume.

The mass, momentum and energy equations for the flow model of the diffuser are:

$$\frac{\partial(\rho_N \epsilon_N u_N A)}{\partial y} = \frac{d\dot{\mathcal{M}}_{\to N}}{dy} \tag{8}$$

$$\frac{dx_N}{dy} = \frac{\Phi(x) - x_N}{\dot{\mathcal{M}}(1+\xi_N)} \cdot \frac{d\dot{\mathcal{M}}_{\to N}}{dy} \tag{9}$$

$$\text{with} \quad \xi_N \equiv \frac{d\dot{\mathcal{M}}_{\to N}}{\dot{\mathcal{M}}_N} \quad \text{and} \quad \Phi(x_N) = \begin{cases} -1, N = C \\ 1, N = D \end{cases}$$

$$\rho_N u_N \epsilon_N A(1+\xi_N)\frac{\partial u_N}{\partial y} + u_N \frac{d\dot{\mathcal{M}}_{\to N}}{dy} = \delta_N(A\frac{dp}{dy} + \frac{f}{8}\pi D\rho u^2) + \frac{\dot{M}_{\to N}}{\delta y} \tag{10}$$

$$\text{with} \quad \delta_N = \begin{cases} 1, N = C \\ 0, N = D \end{cases}$$

$$\frac{\delta\dot{Q}_{\to N}}{\delta y} - \delta_N\left(\frac{f}{8}\pi D\rho u^3\right) = \dot{\mathcal{M}}_N(1+\xi_N)\frac{de_N}{dy} + e_N\frac{d\dot{\mathcal{M}}_{\to N}}{dy} \tag{11}$$

$$\text{with} \quad \frac{de_N}{dy} = \frac{dh_N}{dy} + u\frac{du_N}{dy} \tag{12}$$

The correlations used for the momentum transfer was [8]

$$F_D = -3\pi\rho_C\nu_C u_{CD} D_\delta\left(1 + \frac{3}{16}Re\right) \quad \text{for } Re < 0,5 \tag{13}$$

$$= -3\pi\rho_C\nu_C u_{CD} D_\delta\left(1 + \frac{Re^{\frac{2}{3}}}{6}\right) \quad \text{for } 0,5 < Re < 10^3 \tag{14}$$

$$= \frac{C_D}{2}\rho_C u_{DC}^2 \ \frac{\pi}{4}D_\delta^2 \quad \text{with} \quad C_D = \begin{cases} 0,5, 10^3 < Re < 3\times 10^5 \\ 0,2, Re > 3\times 10^5 \end{cases} \tag{15}$$

with $u_{DC} = u_D - u_C$.

The correlation used for the added mass added force felt by the droplet, at a steady flow, was[8]

$$F_{mass} = -\frac{\rho_C}{12}\pi D_\delta^3 u_D \frac{du_{DC}}{dy}(1 + 2,76\ \epsilon_D) \tag{16}$$

The correlation used for the total ammonia's mass rate transfered from the vapour to each droplet was[7]

$$\dot{\mathcal{M}}/n_D = \pi D\ \overline{Sh}_D\ \rho_C \mathcal{D}_{DC}(x_C - x_D) \qquad \text{with} \quad \overline{Sh}_D = 2 + 0,6Re^{1/2}Sc^{1/3}$$

The correlation used for the total power transfered from the hot droplets to the cold vapour is[7]

$$\dot{Q_D} = \pi D\ k_C(T_D - T_C)\overline{Nu}_D\ n_D \quad \text{with} \quad \overline{Nu}_D = 2 + 0,6Re^{1/2}Pr^{1/3}$$

Some energy will be transfered in the form of the rate of work done by the drag force, which is given by:

$$\dot{W}_{DC} = u_{DC}F_D \tag{17}$$

The droplet diameter variation was

$$\frac{dD_\delta}{D_\delta} \approx \frac{\xi_l}{3} \tag{18}$$

B Design Conditions

The geometrical design conditions are the diameters of the tubes and absorber entry that are to be connected to a future ejector. The ejector is subject to the geometrical conditions described in Tab.1.

	Diameters (mm)
(Entry) Motive fluid (Nozzle)	8
(Entry) Affected fluid	10
(Exit) Absorber (Diffuser's outlet)	10

Table 1: Geometrical Initial Conditions. The measures concern the tube inner diameters.

The chiller, context of this work, functions under specific design working conditions that are described in the following tables.

The nominal conditions for the motive fluid, *i.e.* the weak solution coming from the solution heat exchanger, are in Tab.2.

The nominal conditions for the affected fluid, *i.e.* the ammonia's vapour coming from the refrigerant heat exchanger, are in Tab.3.

Mass flow rate	$\dot{\mathcal{M}}=$	1,62 $\times 10^{-2}$	$kg\ s^{-1}$
Ammonia mass fraction	$x=$	0,432	
Pressure	$p_a=$	15,7	bar
Temperature	$T=$	46,8	°C
Density	$\rho=$	828,2	$kg\ m^{-3}$
Quality	$\mathcal{Q}=$	-0,1 (sub-cooled)	
Ammonia molar fraction	$\mathfrak{x}=$	0,446	
Mean velocity	$u=$	0,39	$m\ s^{-1}$
Sound velocity	$u_s=$	1756,00	$m\ s^{-1}$
Viscosity	$\mu=$	618,5 $\times 10^{-6}$	$kg\ m^{-1}\ s^{-1}$
Reynolds number	$Re=$	4162,0	
Mach number	$Ma=$	2,0 $\times 10^{-4}$	

Table 2: Initial conditions of the motive flow (weak solution).
Indexes: $_a$ indicates that it is the high pressure level.

Mass flow rate	$\dot{\mathcal{M}}=$	2,67 $\times 10^{-3}$	kg/s
Ammonia mass fraction	$x=$	0,985	
Pressure	$p_b=$	5,6	bar
Temperature	$T=$	34,4	°C
Mixture density	$\rho=$	4,1	$kg\ m^{-3}$
Density of the liquid phase	$\rho_L=$	792,9	$kg\ m^{-3}$
Density of the vapour phase	$\rho_V=$	3,9	$kg\ m^{-3}$
Quality	$\mathcal{Q}=$	0,97 (two-phases)	
Ammonia molar fraction	$\mathfrak{x}=$	0,986	
Ammonia mass fraction of the liquid phase	$x=$	0,985	
Ammonia mass fraction of the vapour phase	$y=$	0,998	
Mean velocity	$u=$	8,37	$m\ s^{-1}$
Sound velocity	$u_s=$	427,00	$m\ s^{-1}$
Viscosity	$\mu=$	10,31$\times 10^{-6}$	$kg\ m^{-1}\ s^{-1}$
Volume fraction of the liquid phase	$\epsilon_L=$	0,0001 ≈ 0	
Volume fraction of the vapour phase	$\epsilon_V=$	0,9999 ≈ 1	
Reynolds number	$Re=$	32984,00	
Mach number	$Ma=$	0,02	

Table 3: Initial conditions of the affected flow (refrigerant).
Indexes: $_b$ indicates that it is the low pressure level.